Onboard Carbon Capture and Storage (OCCS) for fossil fuel-based shipping: a Sustainability Assessment

Francesco ZANOBETTI[1], Gianmaria PIO[1], Marta BUCELLI[2], Laura MIANI[1], Sepideh JAFARZADEH[3], Valerio COZZANI[1,*]

[1] LISES – Laboratory of Industrial Safety and Environmental Sustainability, Department of Civil, Chemical, Environmental and Materials Engineering, University of Bologna, Via Terracini 28, 40131, Bologna, Italy

[2] SINTEF Energy Research AS, Sem Sælandsvei 11, 7034, Trondheim, Norway

[3] SINTEF Ocean, Postboks 4762 Torgarden, NO-7465 Trondheim, Norway

*Corresponding Author: valerio.cozzani@unibo.it

Supplementary Material

Section 1. Reference OCCS schemes

S.1.1 Amine scrubbing (AS)

The reference scheme considered for AS-based OCCS separates CO_2 by a continuous reactive absorption-amine solvent regeneration process (Feenstra et al., 2019; Madeddu et al., 2019; Ros et al., 2022). Waste heat associated with the hot exhaust flue gas was considered recovered by a dedicated unit working with diathermic oil as utility fluid. This is ultimately exploited to provide the stripper reboiler heat duty necessary to transfer the captured CO_2 back to the gaseous phase. A direct contact cooling system is used upstream of the capture plant to remove excess water from the gaseous stream while significantly lowering its temperature. Pollutants associated with the flue gas (e.g., SO_x, NO_x, etc.) were found not to require any additional upstream pre-treatment, being their concentration lower than the limits suggested in the literature for effective carbon capture operation (Voldsund et al., 2019). Captured CO_2 collected from the stripper condenser is then subject to multi-stage compression, intercooling and water separation. The number of compression-intercooling-separation units was determined to maintain a pressure ratio per each compression stage as close as possible to an optimal value of 3 (Roussanaly et al., 2013). The highly CO_2-enriched stream is ultimately liquefied using vaporizing LNG as a cold sink. Table S.1 reports the main operating variables assumed to model the reference AS scheme.

Table S.1. Main operating parameters collected for process design of AS-based OCCS scheme.

Parameter	Value	Unit	Reference
	Absorber		
Operating pressure	1.2	bar	(Di Martino et al., 2021)
Operating temperature	40	°C	(Di Martino et al., 2021)
Concentration of MEA in lean solvent	30	wt%	(Madeddu et al., 2019)
Lean loading at the inlet	22	mol_{CO2}/mol_{MEA}-%	(Dutta et al., 2017)
Rich loading at the outlet	47	mol_{CO2}/mol_{MEA}-%	(Dutta et al., 2017)
	Rich/lean heat exchanger		
Minimum temperature approach	10	°C	(Madeddu et al., 2019)
Stripper			
Operating pressure	1.8	bar	(Madeddu et al., 2019)
	Compression and liquefaction		
Single-stage compression pressure ratio	2 – 4 optimal 3	-	(Roussanaly et al., 2013; Voldsund et al., 2017)
Intercooling minimum temperature approach	10	°C	(Voldsund et al., 2019, 2017)
Liquefaction minimum temperature approach	5	°C	(Baccanelli et al., 2016)
Auxiliaries			
Blower/compressor isentropic efficiency	85	%	(Voldsund et al., 2019, 2017)
Pump isentropic efficiency	80	%	(Voldsund et al., 2019, 2017)

S.1.2 Advanced cryogenic carbon capture (A3C)

Cryogenic-based onboard carbon capture was considered performed according to the Advanced Cryogenic Carbon Capture (A3C) (Font-Palma, 2021; Willson et al., 2019) process concept. The hot exhaust flue gas is first cooled against seawater and then sent to a separator to collect condensed liquids. A chiller was considered installed to remove most of the gaseous water at a temperature of about 274 K (Willson et al., 2019). The residual water vapour and CO_2 in the flue gas are then removed in respectively the cooler-drier and desublimer by deposition as frost on the surface of a moving bed of chilled metallic beads. In the sublimer, the packed bed carrying the CO_2 frost is ultimately heated to release CO_2. More specific information on A3C process design can be found elsewhere (Font-Palma, 2021; PMW Technology, 2019; Willson et al., 2019). No additional pre-treatment targeting pollutant emissions was required upstream the capture plant, as already mentioned in Section S.1.1. The procedure adopted to build the sub-flowsheet for compression and liquefaction results the same as previously described for AS. An additional heat recovery step was considered prior to the first compression stage in order to further cool down the CO_2 stream entering the condenser (Font-Palma, 2021; Willson et al., 2019). CO_2 conditioning was found not to require any vapour-liquid separation, in view of the highly dried CO_2 stream provided by the A3C process. The main operating parameters collected to define the A3C scheme are reported in Table S.2.

Table S.2. Main operating parameters collected for process design of the reference A3C scheme.

Parameter	Value	Unit	Reference
	Chiller		
Operating temperature	1	°C	(Willson et al., 2019)
	Cooler-drier		
Operating temperature	-99	°C	(Willson et al., 2019)
Water ice deposition per mass of packing bed	0.1%	kg_{ice}/kg_{bed}	(Willson et al., 2019)
Operating pressure	1	atm	(Willson et al., 2019)
	Desublimer		
CO_2 frost deposition per mass of packing bed	1%	kg_{frost}/kg_{bed}	(Willson et al., 2019)
Operating pressure	1	atm	(Willson et al., 2019)
	Sublimer		
Operating temperature	200	K	(Madeddu et al., 2019)
Operating pressure	1	atm	(Willson et al., 2019)
	Compression and liquefaction		
Single-stage compression pressure ratio	2 – 4 optimal 3	-	(Roussanaly et al., 2013; Voldsund et al., 2017)
Intercooling minimum temperature approach	10	°C	(Voldsund et al., 2019, 2017)
Liquefaction minimum temperature approach	5	°C	(Baccanelli et al., 2016)
	Auxiliaries		
Blower/compressor isentropic efficiency	85	%	(Voldsund et al., 2019, 2017)
Pump isentropic efficiency	80	%	(Voldsund et al., 2019, 2017)

S.1.3 Membrane separation (MS)

A two-stage process concept was considered for the definition of the reference membrane separation-based OCCS scheme. The exhaust flue gas is slightly pressurised and moved to a cooling-water separation unit. Concerning CO_2 capture, the clean flue gas is collected from the high-pressure side of the first membrane stage, while the CO_2-depleted off-gas from the second stage is fully recycled to enhance CO_2 purity in the captured stream (Oh et al., 2022). Vacuum pumps are installed to reestablish trans-membrane pressure difference for separation in the second stage and atmospheric conditions for the outlet captured CO_2 stream. Same assumptions as AS and A3C processes were adopted for the specification of pollutant abatement and compression/liquefaction steps. Table S.3 reports the main operating variables specified for the MS-based OCCS scheme.

Table S.3. Main operating parameters assumed to model the reference two-stage membrane-based OCCS scheme.

Parameter	Value	Unit	Reference
Membrane process			
Feed pressure	1	bar	(Oh et al., 2022)
Vacuum pump pressure ratio	20	-	(Oh et al., 2022)
CO_2 permeance	1000	GPU	(Oh et al., 2022; Xu et al., 2019)
CO_2/N_2 selectivity	50	-	(Oh et al., 2022; Xu et al., 2019)
O_2/N_2 selectivity	5	-	(Oh et al., 2022; Xu et al., 2019)
CO_2/H_2O selectivity	0.8	-	(Xu et al., 2019)
Compression and liquefaction			
Single-stage compression pressure ratio	2 – 4 optimal 3	bar/bar	(Roussanaly et al., 2013; Voldsund et al., 2017)
Intercooling minimum temperature approach	10	°C	(Voldsund et al., 2019, 2017)
Liquefaction minimum temperature approach	5	°C	(Baccanelli et al., 2016)
Auxiliaries			
Blower/compressor isentropic efficiency	85	%	(Voldsund et al., 2019, 2017)
Pump isentropic efficiency	80	%	(Voldsund et al., 2019, 2017)

S.1.4 Pressure swing adsorption (PSA)

Reference OCCS scheme implementing pressure swing adsorption was defined as suggested by Ho et al. (2008) for post-combustion applications. Two parallel fixed packed beds are considered for PSA and operated alternatively according to a four-step Skarstrom cycle, based on pressurization of the adsorbing bed, CO_2 adsorption, depressurization, and evacuation of the adsorbed CO_2. The inlet flue gas is first compressed up to the adsorption operating pressure. A sequence of cooling-water separation steps allows to reduce the flue gas temperature while collecting condensed wastewater. A molecular sieve-based dehydration unit was considered for complete water removal ahead of the PSA unit (Ho et al., 2008). $DeNO_x$ and $DeSO_x$ steps were not required, as stated in section S.1.1, whilst compression and liquefaction unit does not include water separation due to the already dry CO_2 stream exiting the capture process. The assumption adopted for defining operating conditions of PSA-based OCCS are reported in Table S.4.

Table S.4. Main operating parameters assumed for OCCS by PSA.

Parameter	Value	Unit	Reference
	PSA		
Adsorption pressure	6	bar	(Ho et al., 2008)
Desorption pressure	1	bar	(Ho et al., 2008)
Operating temperature	35	°C	(Ho et al., 2008)
Adsorbent particle diameter	2	mm	(Konduru et al., 2007; Won et al., 2012)
Bulk bed density	750	kg/m^3	(Ho et al., 2008)
Bed porosity	0.348	-	(Ho et al., 2008)
Adsorbent capacity for CO_2	4.65	mol_{CO2}/kg_{ads}	(Ho et al., 2008)
	Compression and liquefaction		
Single-stage compression pressure ratio	2 – 4 optimal 3	bar/bar	(Roussanaly et al., 2013; Voldsund et al., 2017)
Intercooling minimum temperature approach	10	°C	(Voldsund et al., 2019, 2017)
Liquefaction minimum temperature approach	5	°C	(Baccanelli et al., 2016)
	Auxiliaries		
Blower/compressor isentropic efficiency	85	%	(Voldsund et al., 2019, 2017)
Pump isentropic efficiency	80	%	(Voldsund et al., 2019, 2017)

Section 2. Assumptions for OCCS economics modelling

Specific input data assumed in the economic analysis for the reference OCCS schemes are reported in Table S.5.

Table S.5. Assumptions for economic performance assessment of reference OCCS schemes.

Parameter	Value	Unit	Reference
	CAPEX		
A3C stainless steel beads	3075	€/tonne	(Towler and Sinnott, 2013)
Liquid CO_2 storage system	2743	€/tonne	(Seo et al., 2016)
	VOPEX		
Electricity	0.119	€/kWh	(Feenstra et al., 2019)
MEA solvent	1862	€/tonne	(Gardarsdottir et al., 2019)
Process water	8.54	€/m^3	(Gardarsdottir et al., 2019)
Glycol solution	3.64×10^{-5}	€/kg	(Willson et al., 2019)

Section 3. Assumptions for OCCS inherent safety assessment

Table S.6 summarises the loss of containment events (LOCs) and corresponding credit factors assessed for the equipment types of interest for OCCS inherent safety assessment (see Section 2.3.4 of the main paper).

Table S.6. Reference loss of containment events (LOCs) and related credit factors assumed for the equipment categories of interest in the analysis (n.c., not considered; n.a., not available).

LOC	Pressurized storage tank/process vessel	Atmospheric storage tank/process vessel	Heat exchanger	Compressor	Pump
R1: small leak, continuous release from a 10 mm equivalent diameter hole	1×10^{-5}	1×10^{-4}	1×10^{-3}	*n.a.*	*n.a.*
R2: catastrophic rupture, release of the inventory in 600 s	5×10^{-7}	5×10^{-6}	5×10^{-5}	*n.a.*	*n.a.*
R3: catastrophic rupture, instantaneous release of the inventory	5×10^{-7}	5×10^{-6}	5×10^{-5}	*n.a.*	*n.a.*
R4: pipe leak, continuous release from a hole having 10% of pipe diameter	*n.c.*	*n.c.*	*n.c.*	1×10^{-3}	5×10^{-4}
R5: pipe rupture, continuous release from the full-bore pipe	*n.c.*	*n.c.*	*n.c.*	1×10^{-4}	1×10^{-4}

The specific threshold values adopted in the analysis to calculate damage distances are reported in Table S.7.

Table S.7. Threshold values considered in the present study, addressing the effects on human targets of the end-point accident scenarios (Iannaccone et al., 2019; Zanobetti et al., 2023).

Accident scenario	Threshold value (effect on humans)
Flash fire	½ LFL [a]
Fireball	7 kW/m^2
Jet fire	7 kW/m^2
Pool fire	7 kW/m^2
Vapor cloud explosion	14 kPa
Physical explosion	14 kPa
Toxic cloud	IDLH [b]

[a] LFL, lower flammability limit [vol%]. [b] IDLH, immediately dangerous to life and health concentration [ppm$_v$].

Section 4. Assumptions for sustainability aggregation

Table S.8 reports the weight factors proposed for the overall sustainability assessment related to different aggregation perspective considered in this analysis.

Table S.8. Sustainability aggregation perspectives adopted in the analysis of the case study for OSI assessment. Weight factors adapted from (Crivellari et al., 2021).

	Weight factors			
Aggregation perspective	Technological performance	Economy	Environment	Society
Individualist	0.05	0.17	0.14	0.64
Egalitarian	0.36	0.08	0.53	0.03
Hierarchist	0.22	0.10	0.58	0.10
Equal weighting	0.25	0.25	0.25	0.25

Section 5. Additional boundary conditions for the case study

Table S.9 reports the exhaust gas data computed for the reference LNG-LBSI system under analysis.

Table S.9. Reference conditions assumed for the exhaust flue gas.

Parameter		Value	Unit
Temperature		380	°C
Pressure		1.01	bar
Flow rate		51.88	kg/s
Composition			
	CO_2	4.9	mol%
	H_2O	9.7	mol%
	N_2	75.0	mol%
	O_2	10.2	mol%
	CH_4	1242	ppm_v
	VOC	151	ppm_v
	NO_x	137	ppm_v
	SO_x	0.4	ppm_v
	PM2.5	0.5	ppm_v

Section 6. Benchmark technologies

S.6.1 Liquid hydrogen-fuelled proton exchange membrane fuel cell (LH_2-PEMFC)

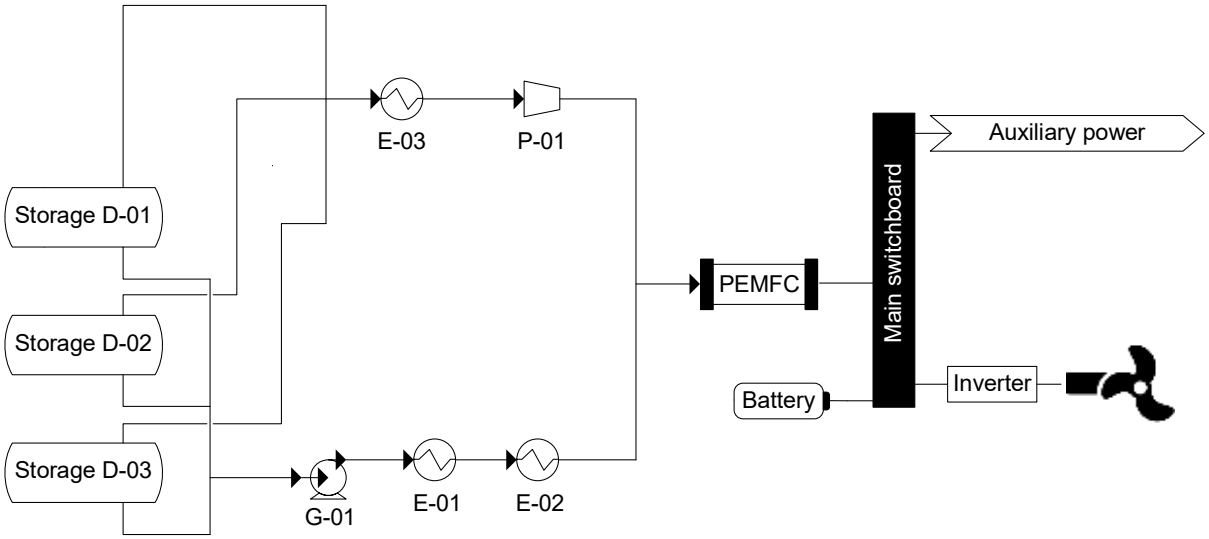

Figure S.1. Reference scheme defined for the benchmark liquid hydrogen-fuelled proton exchange membrane fuel cell (LH_2-PEMFC) technology.

Table S.10. Process operating parameters for the LH_2-PEMFC technology. Units are depicted in Figure S.1.

Parameter	Unit					
	Storage tank (D01-D03)	Pump (G01)	Vaporizer (E01)	Heater (E02)	Boil-off gas heater (E03)	Boil-off gas compressor (P01)
Nominal volume (m^3)	1,200	-	-	-	-	-
Inventory (t)	63.03	-	-	-	-	-
Flow rate (kg/s)	-	0.24	0.24	0.24	4.0×10^{-5}	4.0×10^{-5}
Pressure (bar)	1.0	3.5	3.5	3.5	1.01	3.5
Temperature (°C)	-252.8	-252.4	-247.8	70	-50.6	70
Physical state	Liquid	Liquid	Vapor	Vapor	Vapor	Vapor

S.6.2 Liquid ammonia-fuelled solid oxide fuel cell (LNH_3-SOFC)

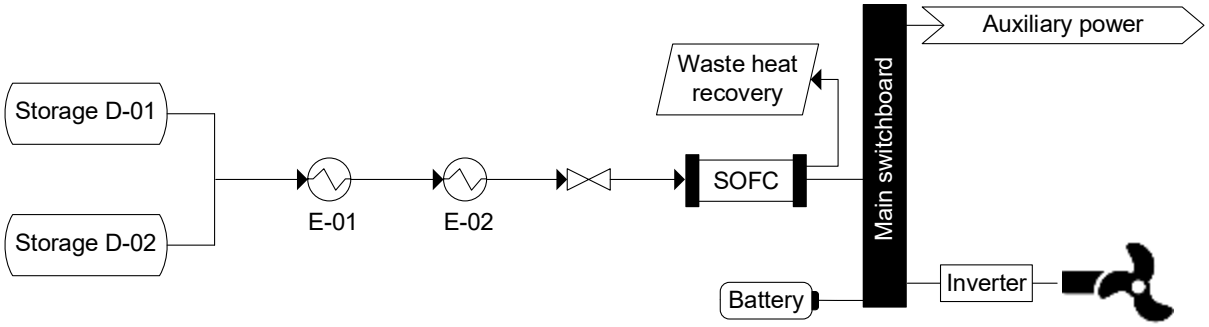

Figure S.2. Reference scheme defined for the benchmark liquid ammonia-fuelled solid oxide fuel cell (LNH_3-SOFC) technology.

Table S.11. Process operating parameters for the LNH_3-SOFC technology. Units are depicted in Figure S.2.

Parameter	Unit		
	Storage tank (D01-D02)	Vaporizer (E01)	Heater (E02)
Nominal volume (m^3)	1,200	-	-
Inventory (t)	558.47	-	-
Flow rate (kg/s)	-	1.46	1.46
Pressure (bar)	8.6	8.6	8.6
Temperature (°C)	20.0	20.3	601.0
Physical state	Liquid	Vapor	Vapor

S.6.3 Liquefied natural gas-fuelled lean burn spark ignition (LNG-LBSI)

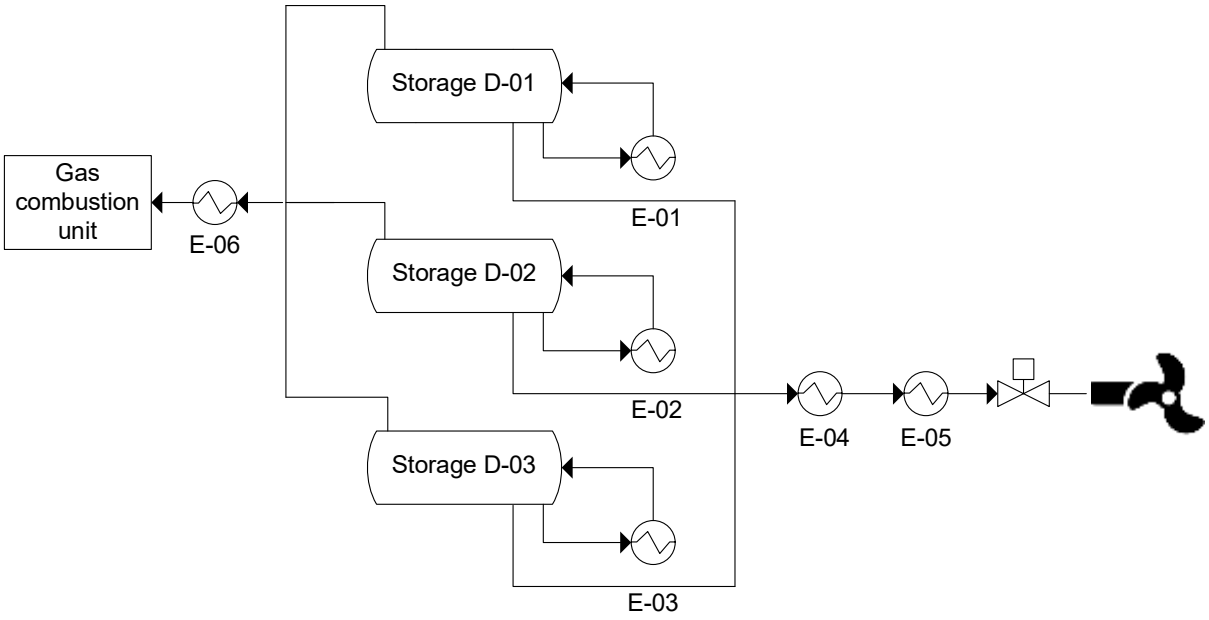

Figure S.3. Reference scheme defined for the benchmark liquefied natural gas-fuelled lean burn spark ignition (LNG-LBSI) technology.

Table S.12. Process operating parameters for the LNG-LBSI technology. Units are depicted in Figure S.3.

Parameter	Unit				
	Storage tank (D01-D03)	Pressure build-up unit (E01-E03)	Vaporizer (E04)	Fuel gas heater (E05)	Boil-off gas heater (E06)
Nominal volume (m^3)	1,200	-	-	-	-
Inventory (t)	495	-	-	-	-
Flow rate (kg/s)	-	0.20	1.62	1.62	6.96×10^{-3}
Pressure (bar)	6.0	6.0	6.0	6.0	6.0
Temperature (°C)	-133.0	-130.0	-123.0	20.0	20.0
Physical state	Liquid	Vapor	Vapor	Vapor	Vapor

References

Baccanelli, M., Langé, S., Rocco, M. V., Pellegrini, L.A., Colombo, E., 2016. Low temperature techniques for natural gas purification and LNG production: An energy and exergy analysis. Appl. Energy 180, 546–559. https://doi.org/10.1016/j.apenergy.2016.07.119

Di Martino, Y., Duque, S.E., Reniers, G., Cozzani, V., 2021. Making the chemical and process industries more sustainable: Innovative decision-making framework to incorporate technological

and non-technological inherently safer design (ISD) opportunities. J. Clean. Prod. 296, 126421. https://doi.org/10.1016/j.jclepro.2021.126421

Dutta, R., Nord, L.O., Bolland, O., 2017. Selection and design of post-combustion CO2 capture process for 600 MW natural gas fueled thermal power plant based on operability. Energy 121, 643–656. https://doi.org/10.1016/j.energy.2017.01.053

Feenstra, M., Monteiro, J., van den Akker, J.T., Abu-Zahra, M.R.M., Gilling, E., Goetheer, E., 2019. Ship-based carbon capture onboard of diesel or LNG-fuelled ships. Int. J. Greenh. Gas Control 85, 1–10. https://doi.org/10.1016/j.ijggc.2019.03.008

Font-Palma, C., 2021. Is Carbon Capture a Viable Solution To Decarbonise the Shipping Industry? TCCS-11 -Trondheim Conf. CO2Capture, Transp. Storage 188–192.

Gardarsdottir, S.O., De Lena, E., Romano, M., Roussanaly, S., Voldsund, M., Pérez-Calvo, J.F., Berstad, D., Fu, C., Anantharaman, R., Sutter, D., Gazzani, M., Mazzotti, M., Cinti, G., 2019. Comparison of technologies for CO 2 capture from cement production—Part 2: Cost analysis. Energies 12, 542. https://doi.org/10.3390/en12030542

Ho, M.T., Allinson, G.W., Wiley, D.E., 2008. Reducing the cost of CO2 capture from flue gases using pressure swing adsorption. Ind. Eng. Chem. Res. 47, 4883–4890. https://doi.org/10.1021/ie070831e

Iannaccone, T., Landucci, G., Scarponi, G.E., Bonvicini, S., Cozzani, V., 2019. Inherent safety assessment of alternative technologies for LNG ships bunkering. Ocean Eng. 185, 100–114. https://doi.org/10.1016/j.oceaneng.2019.05.028

Konduru, N., Lindner, P., Assaf-Anid, N.M., 2007. Curbing the Greenhouse Effect by Carbon Dioxide Adsorption with Zeolite 13X. AIChE J. 53, 3137–3143. https://doi.org/10.1002/aic

Madeddu, C., Errico, M., Baratti, R., 2019. CO2 Capture by Reactive Absorption-Stripping, Editorial Springer.

Oh, J., Anantharaman, R., Zahid, U., Lee, P.S., Lim, Y., 2022. Process design of onboard membrane carbon capture and liquefaction systems for LNG-fueled ships. Sep. Purif. Technol. 282, 120052. https://doi.org/10.1016/j.seppur.2021.120052

PMW Technology, 2019. Decarbonising the Transport System. Evaluation of the Marine Application of Advanced Carbon Capture Technology.

Ros, J.A., Skylogianni, E., Doedée, V., van den Akker, J.T., Vredeveldt, A.W., Linders, M.J.G., Goetheer, E.L.V., G M-S Monteiro, J., 2022. Advancements in ship-based carbon capture technology on board of LNG-fuelled ships. Int. J. Greenh. Gas Control 114. https://doi.org/10.1016/j.ijggc.2021.103575

Roussanaly, S., Jakobsen, J.P., Hognes, E.H., Brunsvold, A.L., 2013. Benchmarking of CO2 transport technologies: Part I-Onshore pipeline and shipping between two onshore areas. Int. J. Greenh. Gas Control 19, 584–594. https://doi.org/10.1016/j.ijggc.2013.05.031

Seo, Y., Huh, C., Lee, S., Chang, D., 2016. Comparison of CO2 liquefaction pressures for ship-based carbon capture and storage (CCS) chain. Int. J. Greenh. Gas Control 52, 1–12. https://doi.org/10.1016/j.ijggc.2016.06.011

Towler, G., Sinnott, R.A.Y., 2013. Chemical Engineering Design: Principles, Practice and Economics of Plant and Process Design. https://doi.org/10.1016/b978-0-08-096659-5.00022-5

Voldsund, M., Anantharaman, R., Berstad, D., Cinti, G., De Lena, E., Gatti, M., Gazzani, M., Hoppe, H., Martínez, I., Monteiro, J.G.M.-S., Romano, M., Roussanaly, S., Schols, E., Spinelli, M., Størset, S., van Os, P., 2017. CEMCAP framework for comparative techno-economic analysis of CO2 capture from cement plants (D3.2).

Voldsund, M., Gardarsdottir, S.O., De Lena, E., Pérez-Calvo, J.F., Jamali, A., Berstad, D., Fu, C., Romano, M., Roussanaly, S., Anantharaman, R., Hoppe, H., Sutter, D., Mazzotti, M., Gazzani,

M., Cinti, G., Jordal, K., 2019. Comparison of technologies for CO 2 capture from cement production—Part 1: Technical evaluation. Energies 12. https://doi.org/10.3390/en12030559

Willson, P., Lychnos, G., Clements, A., Michailos, S., Font-Palma, C., Diego, M.E., Pourkashanian, M., Howe, J., 2019. Evaluation of the performance and economic viability of a novel low temperature carbon capture process. Int. J. Greenh. Gas Control 86, 1–9. https://doi.org/10.1016/j.ijggc.2019.04.001

Won, W., Lee, S., Lee, K.S., 2012. Modeling and parameter estimation for a fixed-bed adsorption process for CO 2 capture using zeolite 13X. Sep. Purif. Technol. 85, 120–129. https://doi.org/10.1016/j.seppur.2011.09.056

Xu, J., Wang, Z., Qiao, Z., Wu, H., Dong, S., Zhao, S., Wang, J., 2019. Post-combustion CO2 capture with membrane process: Practical membrane performance and appropriate pressure. J. Memb. Sci. 581, 195–213. https://doi.org/10.1016/j.memsci.2019.03.052

Zanobetti, F., Pio, G., Jafarzadeh, S., Ortiz, M.M., Cozzani, V., 2023. Inherent safety of clean fuels for maritime transport. Process Saf. Environ. Prot. 174, 1044–1055. https://doi.org/10.1016/j.psep.2023.05.018